

Biosynthesis of the Brevianamides. An *ab Initio* Study of the Biosynthetic Intramolecular Diels–Alder Cycloaddition

Luis R. Domingo,* Juan F. Sanz-Cervera, Robert M. Williams,† M. Teresa Picher, and J. Alberto Marco

Departamento de Química Orgánica, Universidad de Valencia C/ Dr. Moliner 50, E-46100 Burjassot, Valencia, Spain, and Department of Chemistry, Colorado State University, Fort Collins, Colorado 80523

Received November 21, 1996[®]

An *ab initio* study of the transition structures for the intramolecular Diels–Alder cycloaddition of the aza diene **6** to give brevianamides A, **1**, and B, **2**, has been carried out with analytical gradients at *ab initio* 3-21G and 6-31G* basis sets within Hartree–Fock procedures. The correlation effects have been estimated by using the perturbational approach at MP2 and MP3 levels. The geometry, electronic structure, and transition vector component are qualitatively model independent in this study. An analysis of the geometries and energies of the corresponding transition structures provides an explanation for the fact that brevianamide A, **1**, is biosynthesized in larger quantities than brevianamide B, **2**, while their respective epimers at C7 are not formed.

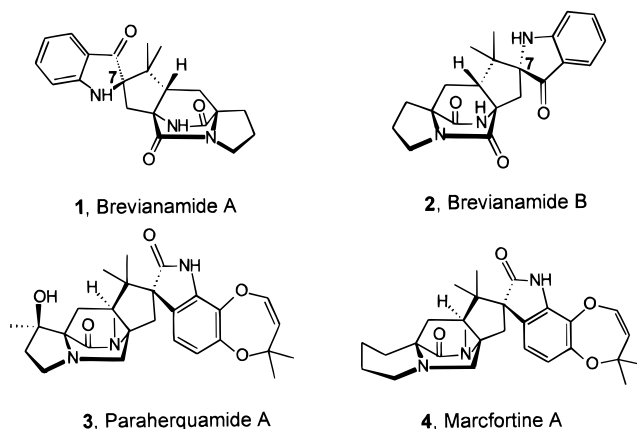
Introduction

While the Diels–Alder reaction is one of the most important ring-forming reactions in organic synthesis, it is surprisingly rare in biosynthetic processes. In the field of natural products, only a few structures have been conjectured to arise through such a cycloaddition reaction,¹ and even in these cases, it is uncertain whether the Diels–Alder reaction is actually operative in their biosynthetic pathways.²

In 1969, Birch and Wright reported the isolation of the first representative of a new class of metabolites from cultures of the fungus *Penicillium brevicompactum*.³ These compounds, called brevianamides, display a structure that could formally originate from a [4 + 2] cycloaddition reaction. The main member of this class, brevianamide A, **1** (Chart 1), was later shown to be present in cultures of the fungi *Penicillium viridicatum*⁴ and *Penicillium ochraceum*.⁵ Subsequent research on these cultures led to the discovery of new members of this class of compounds, brevianamides B³–F.^{6,7} Brevianamides C and D were shown to be isolation artifacts of **1**, for while neither brevianamide C nor D is present in *P. brevicompactum* cultures grown in the dark, irradiation of **1** in solution yields the two compounds.⁷

After the brevianamides were established as a new class of fungal metabolites, two new classes of structurally related compounds were found: the paraherquamides⁸ (paraherquamide A, **3**) and the marcfortines⁹ (marcfortine A, **4**). While **1** has been shown to possess antifeedant effects,¹⁰ several members of the paraherquamide family have a very potent antiparasitic effect,¹¹ as in **3**. In all these compounds, the most distinctive

Chart 1



structural feature is the presence of a diazabicyclo[2.2.2]-octane core that may formally result from a [4 + 2] cycloaddition. It is noteworthy that the relative stereochemistry of the bicyclic ring system in the paraherquamides and marcfortines differs from the one present in the brevianamides in one carbon atom (C-7 in the brevianamide numbering system and C-20 in the paraherquamide numbering system). These facts prompted the study of the biosynthesis of these substances.

(8) (a) Yamazaki, M.; Okuyama, E.; Kobayashi, M.; Inoue, H. *Tetrahedron Lett.* **1981**, 22, 135. (b) Blizzard, T. A.; Marino, G.; Mrozik, H.; Fisher, M. H.; Hoogsteen, K.; Springer, J. P. *J. Org. Chem.* **1989**, 54, 2657. (c) Ondeyka, J. G.; Goegelman, R. T.; Shaeffer, J. M.; Kelemen, L.; Zitano, L. *J. Antibiot.* **1990**, 43, 1375. (d) Liesch, J. M.; Wichmann, C. F. *Ibid.* **1990**, 43, 1380. (e) Blanchflower, S. E.; Banks, R. M.; Everett, J. R.; Manger, B. R.; Reading, C. *Ibid.* **1991**, 44, 492. (f) Blanchflower, S. E.; Banks, R. M.; Everett, J. R.; Reading, C. *Ibid.* **1993**, 46, 1355.

(9) (a) Polonsky, J.; Merrien, M.-A.; Prange, T.; Pascard, C. *J. Chem. Soc., Chem. Commun.* **1980**, 601. (b) Prange, T.; Billion, M.-A.; Vuilhorgne, C. P.; Pascard, C.; Polonsky, J.; Moreau, S. *Tetrahedron Lett.* **1981**, 22, 1977.

(10) (a) Bird, B. A.; Remaley, A. T.; Campbell, I. M. *Appl. Environ. Microbiol.* **1981**, 42, 521. (b) Andersen, B. *Antonie van Leeuwenhoek* **1991**, 60, 115; *Chem. Abstr.* **1992**, 116, 59708d.

(11) (a) Shoop, W. L.; Egerton, J. R.; Eary, C. H.; Suhayda, D. J. *Parasitol.* **1990**, 76, 349. (b) Ostlind, D. A.; Mickle, W. G.; Ewanciw, D. V.; Andriuli, F. J.; Campbell, W. C.; Hernandez, S.; Mochales, S.; Munguira, E. *Res. Vet. Sci.* **1990**, 48, 260. (c) Shoop, W. L.; Michael, B. F.; Haines, H. W.; Eary, C. H. *Vet. Parasitol.* **1992**, 43, 259. (d) Shoop, W. L.; Haines, H. W.; Eary, C. H.; Michael, B. F. *Am. J. Vet. Res.* **1992**, 53, 2032. (e) Schaeffer, J. M.; Blizzard, T. A.; Ondeyka, J.; Goegelman, R.; Sinclair, P. J.; Mrozik, H. *Biochem. Pharmacol.* **1992**, 43, 679.

† Colorado State University.

[®] Abstract published in *Advance ACS Abstracts*, February 15, 1997.

(1) (a) Pindur, U.; Schneider, G. H. *Chem. Soc. Rev.* **1994**, 409. (b) Laschat, S. *Angew. Chem., Int. Ed. Engl.* **1996**, 25, 289.

(2) For some examples of possible biosynthetic Diels–Alder reactions, see: Sanz-Cervera, J. F.; Glinka, T.; Williams, R. M. *Tetrahedron* **1993**, 49, 8471 and references cited therein.

(3) Birch, A. J.; Wright, J. J. *J. Chem. Soc., Chem. Commun.* **1969**, 644.

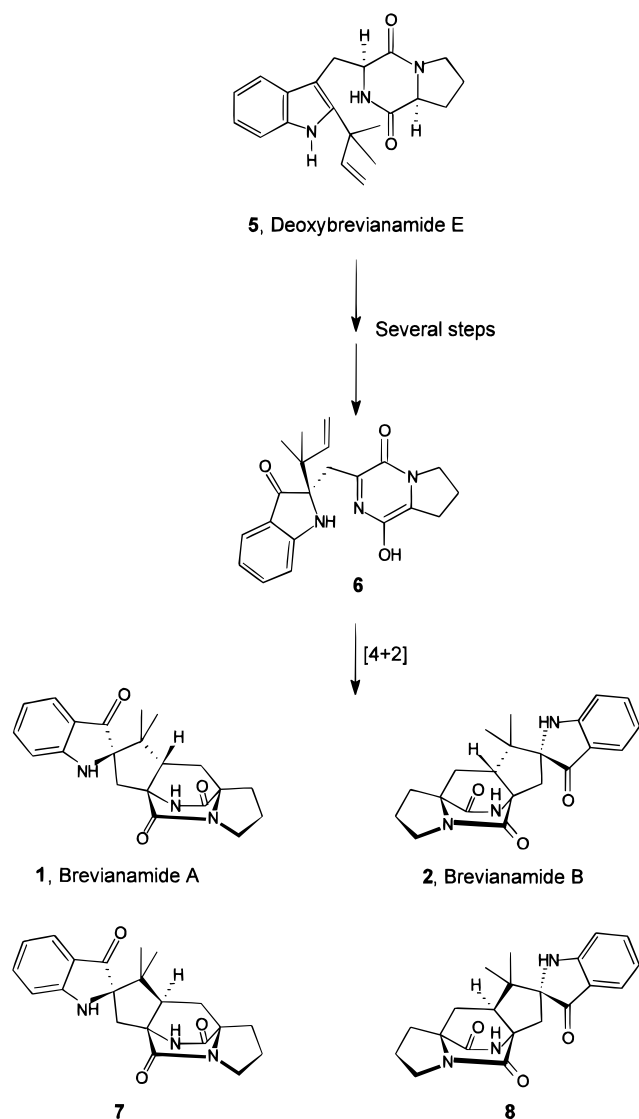
(4) Wilson, B. J.; Yang, D. T. C.; Harris, T. M. *Appl. Microbiol.* **1973**, 633.

(5) Robbers, J. E.; Straus, J. W. *Lloydia* **1975**, 38, 355.

(6) (a) Birch, A. J.; Wright, J. J. *Tetrahedron* **1970**, 26, 2329. (b) Birch, A. J. *J. Agric. Food Chem.* **1971**, 19, 1088.

(7) Birch, A. J.; Russell, R. A. *Tetrahedron* **1972**, 28, 2999.

Scheme 1. Proposed Biosynthesis of Brevianamides A and B (Simplified Scheme)



Following earlier suggestions on the biogenesis of these substances,¹² and in accordance with the results of our own feeding experiments, we have proposed a biosynthetic scheme for the brevianamides,^{2,13} outlined in Scheme 1. According to our proposal, oxidation of deoxybrevianamide E, **5**, followed by a pinacol-type rearrangement and a further oxidation, would yield intermediate key compound **6**. In turn, intramolecular [4 + 2] cycloaddition in compound **6** would yield brevianamides A, **1**, and B, **2**. In principle, this intramolecular cycloaddition could also yield compounds **7** and **8**, which are unknown as natural products.

Considering that compound **6** itself is thus far unknown and that its aza diene system is unusual for a Diels–Alder cycloaddition, it became evident that a theoretical study of this key reaction would provide additional information on the biosynthesis of the brevianamides and the feasibility of a biological Diels–Alder

cycloaddition. To carry out this study, we turned to computational chemical models, which have begun to play an ever increasing role in chemical research, especially concerning the elucidation of molecular reaction mechanisms.

In the present paper, we report an *ab initio* study of the transition structures for the intramolecular Diels–Alder cycloaddition of the aza diene **6** to give **1** and **2** (brevianamides A and B, respectively).

Computational Methods and Molecular Models

All geometry optimizations and gas-phase energy calculations were performed with the Gaussian 92 suite of programs.¹⁴ Unless otherwise specified, all geometries of the reactants and transition structures (TSs) have been fully optimized at the restricted Hartree–Fock (RHF) level with the 3-21G and 6-31G* basis sets.¹⁵ Correlation effects have been estimated using the perturbational approach¹⁶ at MP2/3-21G//HF/3-21G, MP2/6-31G**/HF/6-31G* and MP3/6-31G**/HF/6-31G* levels.

The exact characterization of the transition structures (TSs) was achieved using a simple algorithm¹⁷ in which the set of coordinates describing the system is separated in two, *qi* and *qj*, where *qi* is the control space set responsible for the unique negative eigenvalues in the respective force constant matrix connected with the variables that form the transition vector (TV).¹⁸ The remaining coordinates, set *qj*, is called complementary space. First, the potential energy surface (PES) was explored in the quadratic region of the TS. The transition vector was determined by diagonalizing the force constant matrix, and then the complementary space was optimized. The next step was a complete analytical optimization for the complete space of all variables. This was carried out using the Bery analytical gradient optimization routine.¹⁹ Finally, the nature of the each stationary point was established by analytically calculating and then diagonalizing the matrix of the energy second derivatives to determine the number of imaginary frequencies, zero for local minimum and one for a TS.

Due to the large molecular system of **6** (27 heavy atoms), the present study has been carried out at 3-21G basis set level. For this reason, we chose a simplified model, **9**, in which the essential features of **6** are present (Chart 2), in order to increase the computational level.

Results and Discussion

(I) Study of the Intramolecular Diels–Alder Cycloaddition in Model 9. The study of the intramolecular Diels–Alder cycloaddition in model **9** was carried out using *ab initio* calculations at the 3-21G and 6-31G* basis set levels. Correlation effects have been estimated through the perturbational approach at MP2/3-21G//HF/

(12) (a) Porter, A. E. A.; Sannes, P. G. *J. Chem. Soc., Chem. Commun.* **1970**, 1103. (b) Birch, A. J.; Wright, J. J. *Tetrahedron* **1970**, 26, 2329. (c) Baldas, J.; Birch, A. J.; Russell, R. A. *J. Chem. Soc., Perkin Trans. 1* **1974**, 50.

(13) (a) Williams, R. M.; Kwast, E.; Coffman, H.; Glinka, T. *J. Am. Chem. Soc.* **1989**, 111, 3064. (b) Sanz-Cervera, J. F.; Glinka, T.; Williams, R. M. *J. Am. Chem. Soc.* **1993**, 115, 347. (c) See ref 2.

(14) Gaussian 92, Revision D.2. Frisch, M. J.; Trucks, G. W.; Head-Gordon, M.; Gill, P. M. W.; Wong, M. W.; Foresman, J. B.; Johnson, B. G.; Schlegel, H. B.; Robb, M. A.; Replogle, E. S.; Gomperts, R.; Andres, J. L.; Raghavachari, K.; Binkley, J. S.; Gonzalez, C.; Martin, R. L.; Fox, D. J.; Defrees, D. J.; Baker, J.; Stewart, J. J. P.; Pople, J. A. Gaussian, Inc., Pittsburgh, PA, 1992.

(15) Hehre, W. J.; Radom, L.; Schleyer, P. v. R.; Pople, J. A. *Ab initio Molecular Orbital Theory*; Wiley: New York, 1986.

(16) Pople, J. A.; Seeger, R.; Krishnan, R. Variational Configuration Interaction Methods and Comparison with Perturbation Theory. *Int. J. Quant. Chem. Symp.* **1977**, 11, 149.

(17) (a) Andrés, J.; Moliner, V.; Safont, V. S. *J. Chem. Soc., Faraday Trans.* **1994**, 90, 1703. (b) Tapia, O.; Andrés, J.; Safont, V. S. *J. Chem. Soc., Faraday Trans.* **1994**, 90, 2365. (c) Tapia, O.; Andrés, J. *J. Chem. Phys. Lett.* **1984**, 109, 471.

(18) (a) McIver, J. W., Jr.; Komornicki, A. *J. Am. Chem. Soc.* **1972**, 94, 2625. (b) McIver, J. W., Jr. *Acc. Chem. Res.* **1974**, 7, 72.

(19) (a) Schlegel, H. B. *J. Comput. Chem.* **1982**, 3, 214. (b) Schlegel, H. B. Geometry Optimization on Potential Energy Surface. In *Modern Electronic Structure Theory*; Yarkony D. R., Ed.; World Scientific Publishing: Singapore, 1994; 2 vols.

Table 1. Total Energies (Hartrees), Potential Energy Barriers, and Relative Energies (kcal/mol) for TS1 and TS2

	9	TS1	TS2	ΔE_{TS1}^a	ΔE_{TS2}^a	ΔE_{rel}^b
HF/3-21G	-603.016 679	-602.964 908	-602.957 928	32.49	36.87	4.38
HF/6-31G*	-606.398 057	-606.332 966	-606.325 841	40.85	45.32	4.47
MP2/3-21G//HF/3-21G	-604.257 988	-604.240 331	-604.235 044	11.08	14.40	3.32
MP2/6-31G**/HF/6-31G*	-608.212 506	-608.198 781	-608.192 861	8.61	12.33	3.72
MP3/6-31G**/HF/6-31G*	-608.263 918	-608.227 981	-608.222 140	22.55	26.22	3.67

^a Potential energy barriers relative to **9**. ^b Relative energies of **TS2** relative to **TS1**.

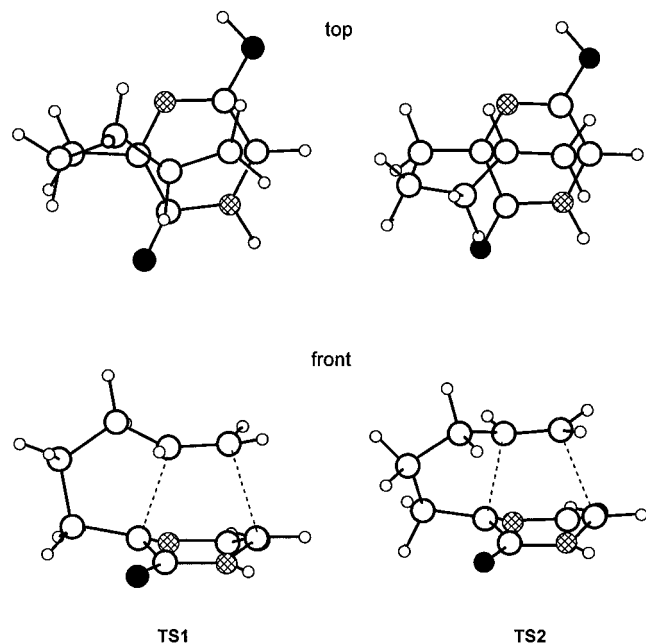
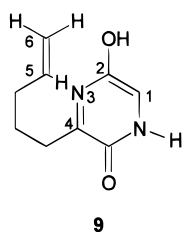


Figure 1. Stereoisomeric transition structures involved in the intramolecular Diels–Alder cycloaddition for model compound **9**.

Chart 2. Model Compound 9 Containing the Azadienic and Vinyl Systems Present in Compound 6



3-21G, MP2/6-31G**/HF/6-31G*, and MP3/6-31G**/HF/6-31G* levels. An exhaustive exploration of the potential energy surface at the 3-21G level of this intramolecular cycloaddition has rendered four TSs: two diastereomeric TSs, **TS1** and **TS2**, and their corresponding enantiomers.

The total energies of the transition structures **TS1** and **TS2** and their potential energy barriers with respect to the reactant are given in Table 1. The 6-31G*-optimized transition structures²⁰ are shown in Figure 1. The selected geometrical parameters of **TS1** and **TS2** are given in Table 2. Similar results were obtained for the enantiomers of **TS1** and **TS2**. The only differences between these enantiomeric TSs are the signs of the dihedral angles and of their corresponding values in the TV. The results obtained using the different procedures are nearly identical.

Table 2. Selected Geometric Parameters for Transition Structures TS1 and TS2 Obtained with HF/3-21G and HF/6-31G* Calculations

	TS1		TS2	
	HF/3-21G	HF/6-31G*	HF/3-21G	HF/6-31G*
C1–C6	2.024	2.193	2.274	2.272
C4–C5	2.209	2.242	2.139	2.153
C1–C2	1.384	1.393	1.382	1.391
C2–N3	1.301	1.295	1.307	1.299
N3–C4	1.340	1.339	1.338	1.338
C1–C6–C5–C4	-19.8	-20.6	2.7	3.9

The values of the potential energy barriers (Table 1) show an important dependency on the calculation level. With the 3-21G basis set, the calculated potential energy barrier for the intramolecular Diels–Alder cycloaddition in model **9** is 32.5 kcal/mol, a value that falls within the calculated range for other intramolecular Diels–Alder reactions described in the literature.²¹ However, when the 6-31G* basis set is used, the potential energy barriers at the RHF level increase notably (40.9 kcal/mol). The inclusion of electron correlation energy at the MP2 level leads to a significant decrease of the potential energy barriers, while the inclusion of electron correlation energy up to the MP3 and MP4 levels leads to reasonable values of the activation parameters.²² This fact shows that MP2 calculations overestimate the effect of the electron correlation energy in transition structures relative to that of the reactants. Consequently, the time-consuming MP3 level is necessary for this reaction. Thus, while MP2/6-31G**/HF/6-31G* calculations decrease the potential energy barrier to 8.6 kcal/mol, MP3/6-31G**/HF/6-31G* calculations give a potential energy barrier for the intramolecular cycloaddition in model **9** of 22.6 kcal/mol.

The relative energies between the two transition structures shown in Table 1 reveal that these are only slightly dependent on the computing level used, falling in a narrow range (3.3–4.4 kcal/mol). These data are in good agreement with the stereoselectivity observed in the formation of the brevianamides A and B relative to their yet to be described epimers at C7.

The bond lengths of C1–C6 and C4–C5 (in the ranges 2.024–2.274 Å and 2.139–2.242 Å, respectively) fall well within the usual range for a Diels–Alder reaction and agree with a concerted mechanism.²¹ For this intramolecular cycloaddition, the transition structures show only slight asynchronicity. When using the 3-21G basis set level, while for **TS1** the forming bond at C1 is shorter than the forming bond at C4 with a $\Delta r = 0.185$ Å, for **TS2** the forming bond at C4 is shorter, with a $\Delta r = 0.135$ Å. González and Houk²³ found a result similar to that for **TS2** in the Diels–Alder reaction of 2-azabutadiene with ethylene. This change in asynchronicity for the intramolecular cycloaddition can be explained by the

(21) Houk, N. K.; Gonzalez J.; Li, Y. *Acc. Chem. Res.* **1995**, *28*, 81.

(22) Jorgensen, W. L.; Lim, D.; Blake, J. F. *J. Am. Chem. Soc.* **1993**, *115*, 2936.

(23) González, J.; Houk, K. N. *J. Org. Chem.* **1992**, *57*, 3031.

(20) Optimized geometries of all the structures are available from the authors.

geometrical strain caused by the formation of the five-membered ring. This effect is evident in the values of the C1–C6–C5–C4 dihedral angles for **TS1** and **TS2** of -19.8° and 2.7° , respectively. The fact that **TS1** has a higher value for this dihedral angle than **TS2** indicates a higher geometrical strain for **TS1** than for **TS2** and explains the change of asynchronicity in the former. In the 6-31G* transition structures the changes are minor compared with those obtained with 3-21G calculations; the lengths of the two forming bonds, C1–C6 and C4–C5, are 2.193 and 2.242 Å and 2.272 and 2.153 Å for **TS1** and **TS2**, respectively, showing a minor asynchronicity.

The arrangement of the vinyl group in relation to the azadienic system is influenced by the simultaneous formation of the five-membered ring, which forces the vinyl group to twist around the forming bonds C–C. Houk *et al.*²⁴ found that, for intramolecular Diels–Alder reactions in which five-membered rings are formed, *cis*-fused products are preferred to *trans*-fused ones. A similar situation is observed in **TS1**, in relation to the alternative **TS2**. However, the preference for the *cis*-fused product (0.7 kcal/mol), obtained with 3-21G calculations for the 1,3,8-nonatriene,²⁵ does not account for the 4.8 kcal/mol obtained for **TS2** in relation to **TS1**. This larger difference in energy between **TS1** and **TS2** can be explained by means of a noneffective overlap between C1 and C6 and C4 and C5 centers in these TSs, caused in turn by the geometrical arrangement of the vinyl group in relation to the azadienic system. In fact, for a hypothetical system derived from **9** by substituting carbon atoms for heteroatoms, 3-21G calculations yield an energy difference of only 1.9 kcal/mol (these calculations are not detailed here).

The 3-21G normal mode analysis of the TSs for model **9** yields a unique imaginary frequency: $695.7i$ ($728.0i$) cm^{-1} and $715.4i$ ($759.1i$) cm^{-1} for **TS1** and **TS2**, respectively (values in parentheses correspond to 6-31G* calculations). These are mainly associated with the formation of C–C bonds. The lowest energy real vibration is a twisting motion of the vinyl group with respect to the aza diene system.

Examination of the transition vector provides the essential details of the chemical process under study.¹⁸ The atomic displacements in the TV correspond to the bond formation step for the Diels–Alder reaction and are associated with the bond lengths C1–C6 and C4–C5, respectively. In addition, the TV shows the change in the bond order for the C1–N2 and C3–C4 bonds (dienic system) and the pyramidalization of C5 and C6 centers (dienophile system).

The values of activation enthalpies, entropies, and Gibbs energies for the intramolecular Diels–Alder reaction of **9** were calculated by means of the potential energy barriers computed at the MP3/6-31G*//RHF/6-31G* level along with the RHF/6-31G* harmonic frequencies.^{22,26} These frequencies were then scaled by 0.9.^{15,22,26} The enthalpy and entropy changes were calculated with standard statistical thermodynamic formulae.¹⁵ The results are presented in Table 3. The inclusion of the zero point energy and the thermal contributions to the barriers leads to a small decrease of the potential energy barriers for both transition structures. The activation

Table 3. Activation Enthalpies (kcal/mol), Entropies (cal/K·mol), and Gibbs Energies (kcal/mol) Calculated at 298.15 K and 1 atm for the Intramolecular Diels–Alder Reaction of **9^a**

	ΔH^\ddagger	ΔS^\ddagger	ΔG^\ddagger
TS1	21.83	–16.09	26.63
TS2	25.48	–15.46	30.08

^a Calculated from MP3/6-31G*//HF/6-31G* electronic energies and the HF/6-31G* vibrational frequencies scaled by 0.9.

entropies for the intramolecular Diels–Alder cycloaddition of **9** are in the range of -15.5 to -16.1 cal/mol·K. The Gibbs activation energies for **TS1** and **TS2** are 26.6 and 30.1 kcal/mol, respectively. The difference between these Gibbs activation energies (3.5 kcal/mol) leads to a ratio of the rate constants for the two reaction channels of *ca.* 340 at 298.15 K, which is consistent with the complete stereoselectivity observed of the brevianamides A and B relative to their yet to be described epimers at C7.

Lewis acid catalysts have a large influence on both the rate and the mechanistic course of Diels–Alder reactions.²⁷ For this reason, the effect of a Lewis acid on the mechanism of the intramolecular Diels–Alder cycloaddition in model **9** has been studied using BH_3 as the Lewis acid model. It has been assumed that the BH_3 is coordinated to the nitrogen atom of the diene system in model **9**. The optimized structures of the model **9**– BH_3 complex and the **TS1**– BH_3 complex were calculated at the 3-21G level, and the energy was computed at the MP3/6-31G*//HF/3-21G level.

The calculated potential barriers are 27.8 and 19.3 kcal/mol at the 3-21G and MP3/6-31G*//HF/3-21G levels, respectively. These calculations predict that the potential energy barrier of the intramolecular Diels–Alder reaction of the model **9**– BH_3 complex is lower by 4.7 and 3.3 kcal/mol than for the parent reaction of model **9**. A similar trend has been found by González and Houk²³ for the cycloaddition reaction of 2-azabutadiene– BH_3 complex and ethylene, which is 6.4 kcal/mol lower. The main change in the transition structure **TS1**– BH_3 complex is a slight increase of asynchronicity; the C1–C6 forming bond is shortened by 0.004 Å, and the C4–C5 forming bond is lengthened by 0.075 Å.

In terms of frontier molecular orbitals, the intramolecular Diels–Alder reaction of model **9** appears to be controlled by the HOMO-1, located mainly in the dienophile system, and the LUMO, located mainly in the aza diene system ($\Delta E_{\text{LUMO-HOMO-1}} = 12.1$ eV and $\Delta E_{\text{LUMO+1-HOMO}} = 13.6$ eV). Thus, the effect of the Lewis acid catalyst is explained by the narrowing of the LUMO–HOMO-1 gap to 11.2 eV.

Although the Gibbs activation energy for the intramolecular Diels–Alder cycloaddition of **9** is somewhat high for the reaction to take place at room temperature, two catalytic factors can be important in lowering this energy under 20.0 kcal/mol: Lewis acids and “entropic traps”.²⁸ This result would agree with a hypothetical enzymatic catalysis in the cycloaddition reaction that leads to brevianamides A and B, as suggested in our proposal for the biosynthesis of these metabolites.^{2,13}

(II) Study of the Intramolecular Diels–Alder Cycloaddition of Aza Diene **6.** In the second part of

(24) Raimondi, L.; Brown, F. K.; Gonzalez, J.; Houk, K. N. *J. Am. Chem. Soc.* **1992**, *114*, 4796.

(25) Lin, Y. T.; Houk, K. N. *Tetrahedron Lett.* **1985**, *26*, 2269.

(26) Houk, K. N.; Loncharich, R. J.; Blake, J. F.; Jorgensen, W. L. *J. Am. Chem. Soc.* **1989**, *111*, 9172.

(27) Jursic, B. S.; Zdravkovski, Z. *J. Org. Chem.* **1994**, *59*, 7732.

(28) Pericyclic reactions with a lower activation enthalpy, as in the Cope and the Claisen rearrangements (*ca.* $\Delta S^\ddagger = -15$ cal/mol·K), display an antibody-catalysis by “entropy trap”. Braisted, A. C.; Schultz, P. G. *J. Am. Chem. Soc.* **1994**, *116*, 211.

Table 4. Total Energies (Hartrees) for 6, TS3, TS4, TS5, and TS6

	3-21G//3-21G	6-31G*//3-21G
6	-1189.90657	-1196.54873
TS3	-1189.85587	-1196.48709
TS4	-1189.84374	-1196.47697
TS5	-1189.83618	-1196.46952
TS6	-1189.83115	-1196.46680

Table 5. Calculated Potential Energy Barriers and Relative Energies (kcal/mol) for TS3, TS4, TS5, and TS6

	3-21G//3-21G		6-31G*/3-21G	
	ΔE_a^a	ΔE_{rel}^b	ΔE_a^a	ΔE_{rel}^b
TS3	31.81	0.00	38.68	0.00
TS4	39.42	7.61	45.03	6.35
TS5	44.17	12.36	49.71	11.02
TS6	47.07	15.26	51.41	12.73

^a Potential energy barriers relative to **6**. ^b Relative energies relative to **TS3**.

this study, the TSs involved in the intramolecular Diels–Alder cycloaddition of biosynthetic key intermediate **6** were studied. The free rotation of the C–C bonds in the dimethylallyl side chain gives rise to a large number of possible conformers, four of which can yield four different diastereomeric cycloaddition adducts (**1**, **2**, **7**, and **8**). We carried out a 3-21G study of the TSs that led to these diastereomeric adducts, and we then compared their energies in an attempt to explain the biosynthetic results: of these four diastereomers, brevianamide A, **1**, is the major natural product, brevianamide B, **2**, is present in much smaller proportion, and **7** and **8** are unknown as natural products.

The total energies of the transition structures **TS3**, **TS4**, **TS5**, and **TS6** are given in Table 4. The calculated potential energy barriers with respect to **6** and the relative energies with respect to **TS3** are given in Table

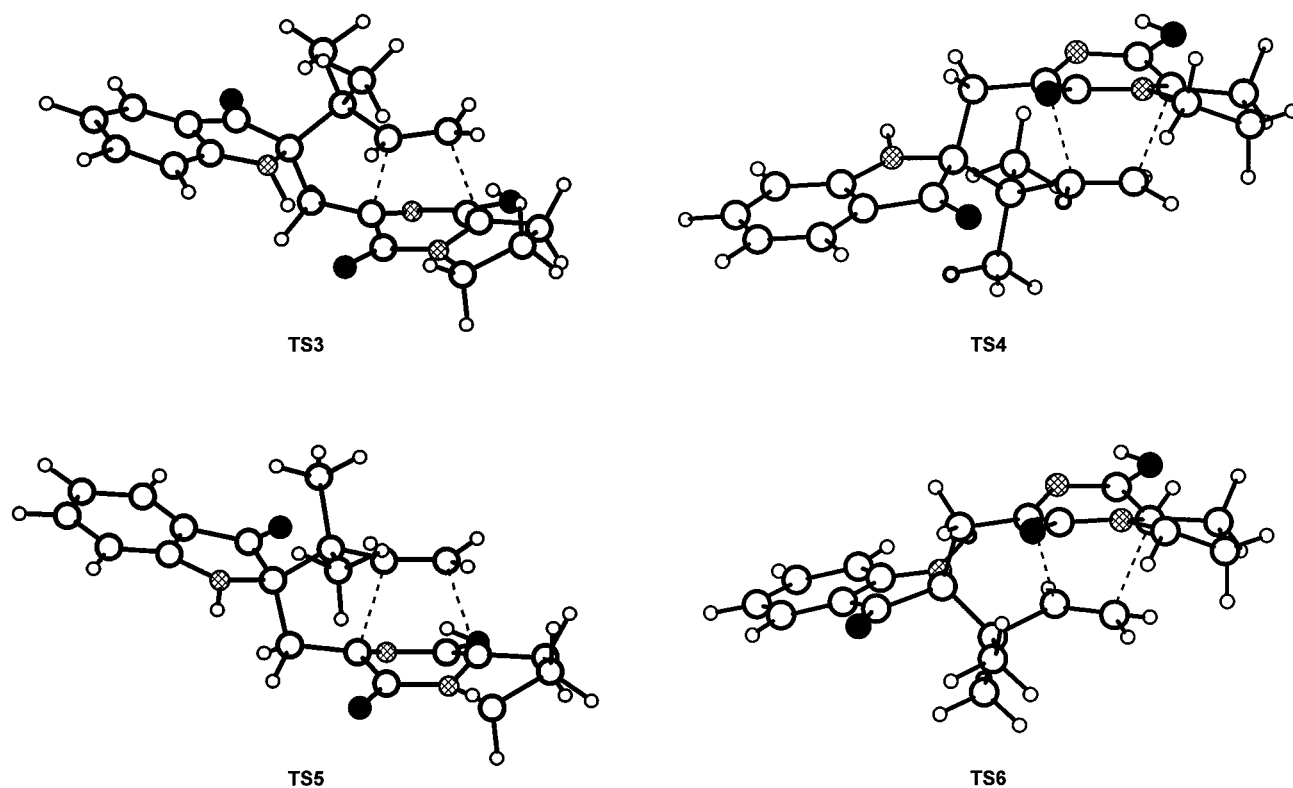
Table 6. Selected Geometric Parameters for Transition Structures TS3, TS4, TS5, and TS6 Obtained with HF/3-21G Calculation

	TS3	TS4	TS5	TS6
C1–C6	2.203	2.260	2.273	2.243
C4–C5	2.196	2.167	2.153	2.164
C1–C2	1.388	1.381	1.386	1.390
C2–N3	1.295	1.300	1.299	1.230
N3–C4	1.348	1.345	1.348	1.355
C1–C6–C5–C4	-27.3	21.9	13.3	-11.2

5. Figure 2 shows the 3-21G-optimized geometries obtained for the TSs that lead to brevianamides A, **1**, **B**, **2**, and their stereoisomers **7** and **8**. Selected geometrical parameters of these TSs are given in Table 6.

The 3-21G and 6-31G* potential energy barriers for the diastereomeric structures **TS3**, **TS4**, **TS5**, and **TS6** (Table 5) turned out to be similar to those obtained for model **9** (Table 3). Furthermore, they allowed a distinction between the structures **TS3** and **TS4** (potential barriers at 3-21G level: 31.8 and 39.4 kcal/mol, respectively) and the structures **TS5** and **TS6** (44.2 and 47.1 kcal/mol respectively). While the transition structures **TS3** and **TS4** lead to the observed biosynthetic products, brevianamides A, **1**, and B, **2**, the transition structures **TS5** and **TS6** would lead to stereoisomers **7** and **8**, which are unknown as natural products. This difference of energy may be explained in terms of the higher energy contents of the last two TSs, caused by the positioning of the vinyl group relative to the aza diene system, which is in turn influenced by the formation of the five-membered ring during the reaction.

Moreover, the differences of potential energy barriers for the transition structures **TS3** and **TS4**, which lead to brevianamides A, **1**, and B, **2**, respectively, can be explained by means of the different arrangement of the amine group in the indoxyl system with respect to the

**Figure 2.** Stereoisomeric transition structures involved in the intramolecular Diels–Alder cycloaddition of compound **6**. **TS5** and **TS6** lead to the formation of brevianamides A and B, respectively.

carbonyl group in the aza diene ring. In **TS3** the hydrogen of the amine group is close enough to the oxygen of the carbonyl group (1.994 Å) to form a hydrogen bond, whereas in **TS4** this interaction is not possible. This stereoelectronic effect found in the gas-phase calculations explains why the potential energy barrier for **TS3** is lower in 6.4 kcal/mol than for **TS4** and provides an explanation for the fact that the formation ratio for brevianamides A, **1**, and B, **2**, in their biosynthesis is approximately 20:1.

The lengths of the bonds formed during the course of the cycloaddition reaction fall within the range 2.153–2.273 Å. These results are similar to those obtained for model **9**, showing also a slight asynchronicity. For these TSs all C1–C6 forming bonds (in the range 2.203–2.273 Å) are longer than the C4–C5 forming bonds (in range 2.153–2.196 Å), in agreement with the results obtained for the Diels–Alder reaction of 2-azabutadiene with ethylene.²³

The normal mode analysis of these transition structures yields a unique imaginary frequency (678*i*, 673*i*, 715*i*, and 753*i* cm⁻¹ for **TS3**, **TS4**, **TS5**, and **TS6**, respectively) which is principally associated with the formation of the C1–C6 and C4–C5 bonds. These results are similar to those obtained for **TS1** and **TS2**.

The results of the study of the TVs for the four possible TSs are quite similar to those obtained for the TS corresponding to the cycloaddition reaction of model **9**. The atomic displacements in the TV correspond to the bond formation step of the Diels–Alder reaction and are associated with the bond lengths C1–C6 and C4–C5, respectively. The TV also shows the change in the bond order for the C1–N2 and C3–C4 bonds (dienic system) and the pyramidalization of the C5 and C6 centers (dienophile system).

Conclusions

This *ab initio* study reveals that brevianamides A and B may be formed through an intramolecular Diels–Alder cycloaddition of the proposed biosynthetic key 2-azabutadiene intermediate. The relative energies of the different TSs are caused mainly by the different orientation of the vinyl group in relation to the aza diene system. In turn, this orientation is influenced by the formation of the five-membered ring. These combined factors explain why only brevianamides A and B are biosynthesized, but not their epimers in C7. In addition, the different arrangement of the amine group in the indoxyl system with respect to the carbonyl group in the azadiene ring with formation of a intramolecular hydrogen bond explains why in the biosynthesis of A and B the former is the main product.

Moreover, the theoretical study of the thermodynamic activation parameters for this biosynthetic intramolecular Diels–Alder cycloaddition shows that coordination of the 2-azabutadiene system with a Lewis acid or “entropic trap” catalysts can decrease the Gibbs activation energy, allowing the reaction to take place under biological conditions.

Acknowledgment. The authors would like to thank Prof. J. Andrés for helpful comments as well as the Servei d'Informàtica of the Universitat Jaume I for providing CPU time on their workstations. We also would like to thank Laura J. Gatzkiewicz for editing the English manuscript. J.F.S.-C. and J.A.M. thank the DGICYT of Spain for financial support (project PB95-1089). R.M.W. acknowledges financial support from the National Science Foundation and from the donors of the Petroleum Research Fund, administered by the ACS.

JO9621783